Fano core resonances and augmented continua of Zn adsorbed on and dissolved in alkali metals

T.-H. Chiu* and C. P. Flynn
Department of Physics and Materials Research Laboratory, University of Illinois at Urbana-Champaign, Urbana, Illinois 61801
(Received 11 September 1985)

We report $3d^{10}4s^2 \rightarrow 3d^9 4s^2 4p$ excitation spectra of Zn impurities coupled to alkali-metal host lattices. Very similar effects are observed for Zn adsorbed on alkali-metal surfaces and dissolved in the bulk of alkali-metal host lattices. Much of the $3d \rightarrow 4p$ oscillator strength occurs in a broad absorption continuum. A remaining sharp fraction of the process interferes with the continuum with a decay lifetime of ~ 0.5 eV, which exceeds the value for autoionization of the free Zn atom by only a factor ~ 2. There is evidence that the $D_{3/2}$ and $D_{5/2}$ hole channels interfere. In its weak resonance amplitude and strong continuum absorption the $3d \rightarrow 4p$ process resembles the $4s \rightarrow 4p$ process reported in an earlier publication. In both processes, the resonance (per Zn atom) weakens markedly as the Zn concentration is increased. These observations are discussed in the light of theoretical models.

I. INTRODUCTION

This paper describes an experimental investigation of the electronic excitation spectra of Zn impurities adsorbed on and dissolved in simple-metal host lattices. In an effort to be fairly comprehensive the chosen substrates for adsorbate studies include Cs, Rb, K, Na, Li, and Mg. Only Na and Rb were investigated as hosts for dilute alloys, and then with some difficulty. Of principal concern here are the $3d^{10}4s^2 \rightarrow 3d^9 4s^2 4p$ excitations of Zn atoms coupled to the metallic environment. The choice of impurity excitations was governed by several factors related to the atomic excitations and to the metallic host. These connections will be explained in what follows, before experimental details are presented.

Excitations of atomic Zn are particularly interesting near the $3d$ threshold. It happens that the $3d^{10}4s^2 \rightarrow (3d^{10}4s)^+$ ionization continuum begins near 9.4 eV.[1] The main $3d^{10}4s^2 \rightarrow 3d^9 4s^2 4p$ excitations, which occur near 11.4 eV, are, of course, degenerate with this $4s \rightarrow 4p$ continuum channel. The two interfere to produce unusual line shapes which are further complicated by interference between the $D_{3/2}$ and $D_{5/2}$ $3d$ hole channels.[2] The interferences indicate that the wave functions for the different channels are connected by Coulombic matrix elements, so that, for example, the local state decays into the continuum over the course of some time interval $\sim 10^{-14}$ sec. As a consequence, the main $3d \rightarrow 4p$ resonance of atomic Zn is broadened to a width of about 0.2 eV but, in addition, exhibits a central dip which is both sharp and very deep. Semiquantitative theories which describe this behavior quite well have appeared.[3] The primitive interference process in autoionization was described by Fano and Cooper.[4]

Continua are encountered in solid-state spectra more frequently than in atomic spectra.[5] In metals, for example, the continuum of single electron-hole pair excitations extends from zero to all higher energies. Much the same phenomena also appear in insulators above their fundamental band gaps. Spectra of local states appear, as a matter of course, superposed on "background" continua in x-ray photoelectron spectroscopy, ultraviolet photoelectron spectroscopy, photon absorption, and emission spectroscopies, and so on. So much is this the case that routine "background subtractions" are employed before the remaining line profile is compared with detailed theories. No account is generally taken of possible nonadditivity between the local and continuum channels, such as that produced by interference processes. It is nevertheless well known that Auger-like decay is the dominant channel for core deexcitation in solids.[6,7] In such processes the initial core-hole energy is transformed into valence-electron excitations of the final state. These are precisely the solid-state equivalent of the autoionizing decays responsible for the Fano-Beutler interferences of free atoms. Continuumlike features can also be introduced into the spectra of both atomic and solid-state systems by Coster-Kronig processes in which one core hole decays into a second hole state by an Auger-like process.[7,8]

Several examples in which a core excitation interferes with a continuum have nevertheless been recognized. These include cases of loss spectroscopy,[9] optical absorption,[10] photoemission,[11] and ellipsometric studies.[12] Of these, the absorption and ellipsometric work bear the closest relationship to the experiments reported in this paper. They are discussed briefly here.

In optical transmission measurements on halogen ions alloyed at dilution into alkali-metal host lattices, Avci and Flynn[10] report observation of substantial impurity-induced absorption continua in the (5—12)-eV range of photon energies. This absorption spreads far beyond the normal Drude range.[13] Halogen $(np^6)^- \rightarrow (np^5)^0$ charge-transfer excitations are observed as spin-orbit-split shoulders which occur at accurately predictable energies. A prethreshold dip is apparent where the local process interferes with the continuum. In all cases the amplitude of

the threshold process per halogen ion increases noticeably with decreasing concentration, thereby indicating that each halogen reduces the oscillator strength accessible to its neighbors. For F, in particular, the resonance is reduced almost entirely to a window in the continuum. This is no doubt due to the fact that the small F^- ion of the initial state lacks overlap with the conduction electrons screening the F^0 atom of the final state.[10,14]

Still more closely related to the Zn case are investigations of divalent metals dissolved in Li, which employed ellipsometric methods in the photon-energy range 1.5–5 eV.[12] The Zn $4s^2 \rightarrow 4s4p$ excitations, red-shifted to near 2.5 eV, were observed on a very strong Drude-like background continuum which falls off with increasing photon energy. Like the halogen-ion excitations (but unlike the Mg $3s^2 \rightarrow 3s3p$ excitation, which is red-shifted to about 2.8 eV), the Zn $4p$ resonance weakens as the concentration of Zn impurities is increased. It eventually becomes submerged in the sloping continuum for Zn concentrations near 10 at.%. The character of the background at low energy prevents any unambiguous identification of interference with the local process. The presence of a strong Auger-like decay channel may nevertheless be deduced from the general width ~ 1 eV of the resonance. In comparison, the expected lifetime against photon emission corresponds to a width $\sim 10^{-8}$ eV. The strong likelihood of an interference between the local process and the continuum may therefore be inferred.

Zn was chosen for study in the present work because both the alloy research at $\hbar\omega < 5$ eV (Ref. 12) and the atomic results above 10 eV (Ref. 2) reveal continua and interferences with local processes. The Zn $3d$ excitation offers the opportunity to examine the impurity-induced continuum at higher energy and the way the atomic interference is modified by the solid-state environment. Moreover, the same excited orbital is involved in both the $3d \rightarrow 4p$ resonance and the $4s \rightarrow 4p$ resonance, so the opportunity arises to search for common features associated with the $4p$ state itself. Several previous investigations of Zn excitations have been reported. The work includes photoemission studies[15] of pure Zn and Zn impurities,[16] and also optical investigations.[17]

In what follows, Sec. II summarizes the experimental methods employed in this research and Sec. III presents the experimental results. Section IV discusses the data and the electronic structure from which the observed behavior originates. A brief report which summarizes this work has appeared earlier.[18]

II. APPARATUS AND TECHNIQUES

The experiments reported below employ differential reflectance spectroscopy using synchrotron radiation. Details of the equipment have been described elsewhere.[19] The monochromatized synchrotron output is chopped into two alternating parallel beams by double reflections, and these beams reflect from the signal and reference areas of the substrate, respectively, to a common detector. Source and detector drift are thereby eliminated from the fractional difference between the channels. Two specimen areas are deposited *in situ* with fresh Mg or Al to make the primary reflector, and the two samples prepared on top by dual-beam methods. In the case of alloys, the host metal covers both substrate areas at once while the doping beam simultaneously falls on the signal area alone. For adsorbates, the surface doping occurs *after* the host metal film is prepared. Successively heavier adsorbate dopings can be created on the same substrate. In both alloy and surface studies a reference run is made before sample preparation to eliminate minor imbalance between channels. These methods provide a spectroscopy sensitive, in general, through the photon-energy range 0–22 eV. The use of CsI as a photocathode limited the useful range in the present experiments to energies greater than about 7.5 eV.

Liquid-He temperatures are an essential feature of this work. Alkali-metal alloys evolve thermally, even below 25 K,[20] and similar behavior is expected for adsorbates on alkali-metal surfaces. Therefore the materials configurations on which the research focuses can neither be prepared reliably nor investigated at higher temperatures. In addition, the cryohead is fitted with He temperatures and intermediate-temperature oxygen-free high-conductivity (OFHC) copper cans which surround the sample and provide extremely-high-speed cryopumping near the sample. This has particular value for the handling of materials as reactive as the alkali metals in experiments which require surfaces free from contamination. In the present work a Helitran cold tip provided the necessary cooling. The experimental arrangement is described in more detail elsewhere.[19] The methods employed to establish that the results are characteristic of clean samples, lacking surface contamination, are also described.[21]

A second important part of this research was the use of clean, reliable sources of molecular beams for metal deposition. The device used for heavy alkali metals allowed the intact sealed glass ampoules to be broken and handled thereafter under conditions of ultrahigh vacuum. This prevents the growth of volatile oxides which may later be transferred to the substrate by evaporation. A detailed description of these sources is available in the literature.[21] Boat sources were preferred for Li because of its higher melting temperature and lower reactivity. Zn was sublimed from a carefully cleaned sample held in a tungsten heating coil. All sources were degassed before use and were operated for some time before sample preparation, to ensure optimal conditions. Sample beams were confined by Cu shields at nitrogen or lower temperature to prevent the spread of low-vapor-pressure metals throughout the bell jar. Those portions of the beams which reached the substrate during sample preparation passed through holes otherwise blocked by He temperature shutters. Quartz-crystal monitors at low temperature were employed to record the beam fluxes. These monitors were accurately calibrated in auxiliary experiments. The low temperature eliminated composition and coverage uncertainties which could otherwise arise from reevaporation or through the departure of sticking coefficients from unity.

It has been established in other work[19,22] that differential reflectance measurements of the type employed here can give spectra fairly accurately proportional to the imaginary (absorptive) part of the thin-film response. For

the energy range of interest here this is particularly the case for Mg substrates, which accordingly were used throughout the research. A second requirement is that the active films which cover the primary reflector must be reasonably transparent. In the present work the alkali metals employed as substrates were therefore restricted to thicknesses ~ 100 Å. Zn adsorbates were examined by reflection in p-polarized light at various coverages which were achieved by successive Zn additions to the same surface. Alloys were prepared as films, also < 100 Å thick, and examined in s polarization owing to the configuration required for sample preparation. Zn coverages up to a few monolayers, and alloys up to a few atomic percent Zn concentration, constitute a fairly small perturbation on the optical propagation, and should therefore fall within the range in which the differential signal remains reasonably proportional to the Zn absorption. The spectra reported in Sec. III are subsequently interpreted on this basis.

III. RESULTS

In this work we are concerned with optical signals arising from Zn adsorbed on and alloyed into alkali-metal films. As the signals vary in approximate proportion to the surface coverage of Zn, it is convenient to eliminate this primary effect by scaling the data to show the signal *per Zn atom*. The figures that follow therefore provide absolute spectra of $-\Delta R/R\Theta$, viz., the fractional reflectivity reduction caused by absorption, scaled by coverage, with coverage measured in atoms cm^{-2}. In all cases the results refer to a sample temperature of about 10 K.

An example which exhibits many of the relevant features is provided by Zn adsorbed on the Mg reflector itself. Figure 1 shows results for Zn on Mg at five coverages between 1.8×10^{14} and 5.4×10^{15} cm^{-2}. Additional results presented in Fig. 2 are spectra taken with a LiF filter placed in the optical path to eliminate spurious effects of possible higher-order light from the monochromator. The data in Fig. 2 are therefore confined to energies below the LiF cutoff near 12 eV. The important point established by a comparison of Figs. 1 and 2 is that second-order–light problems are negligible for the Mg substrate.

Four features of the Zn spectrum on Mg are common to much of what follows. First, Zn introduces an absorption continuum extending from the lower limit of measurement near 7.5 eV to all higher energies. Second, the Zn $3d^{10}4s^2 \rightarrow 3d^9 4s^2 4p$ excitation appears near $\hbar\omega = 9.5$ eV mainly as an asymmetrical dip in the continuum. This is readily recognized as resembling a Fano process of interference between the continuum absorption and the Zn local excitation. Third, unambiguous evidence of the Zn spin-orbit splitting can be discovered in the inflection visible on the high-energy shoulder of the dip, just below 10 eV. Fourth, the size of the signal, normalized for coverage, increases markedly with decreasing coverage. The increase remains, however, much less than the coverage change of a factor ~ 30.

It may be remarked that the continuum absorption present in the spectra is, in general, difficult to measure with absolute accuracy. The differential form of the

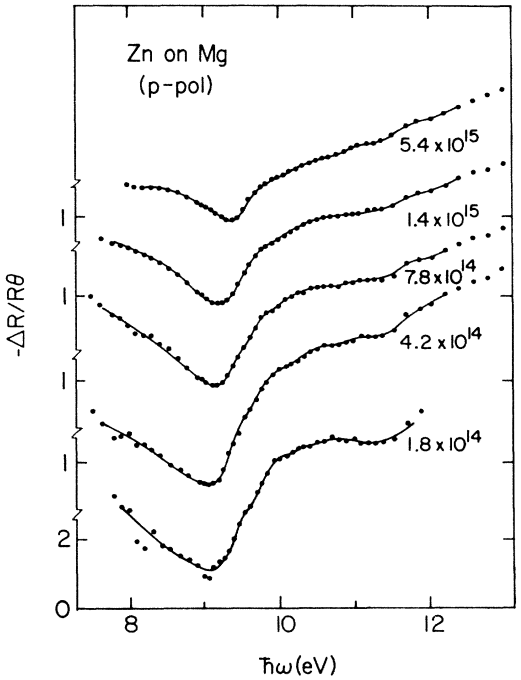

FIG. 1. Fractional reflectivity change caused by Zn impurities adsorbed on Mg at various coverages. The spectra are shown normalized as $\Delta R/R\Theta$ for easy comparison of oscillator strengths, with coverage Θ in units of 10^{14} cm^{-2}.

equipment is intended to eliminate spurious imbalances between channels and focus attention on wavelength-dependent features. Accordingly, residual small differences of uncertain origin are not ordinarily of concern. In the present case, however, the effects scale systematically

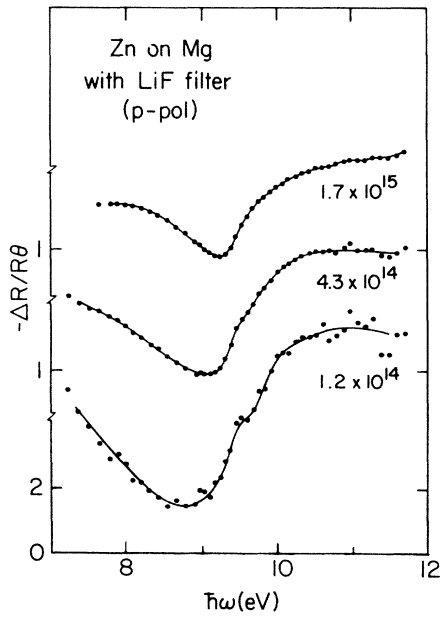

FIG. 2. Fractional reflectivity change, normalized as in Fig. 1, caused by Zn impurities adsorbed on Mg at various coverages. A LiF filter was employed to eliminate second-order light, but the comparison with Fig. 1 reveals no effect from this cause.

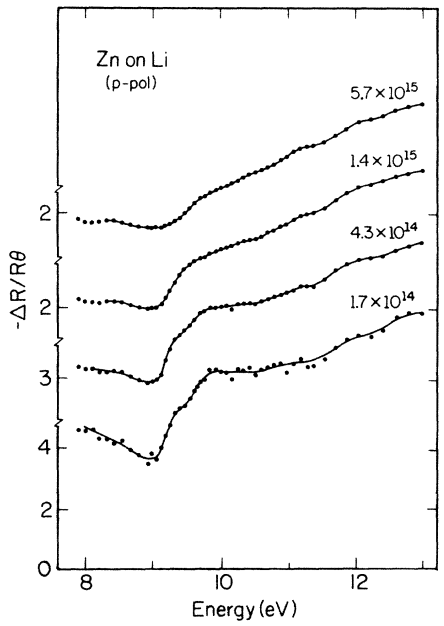

FIG. 3. Fractional reflectivity change, normalized as in Fig. 1, caused by impurities adsorbed on Li at various coverages.

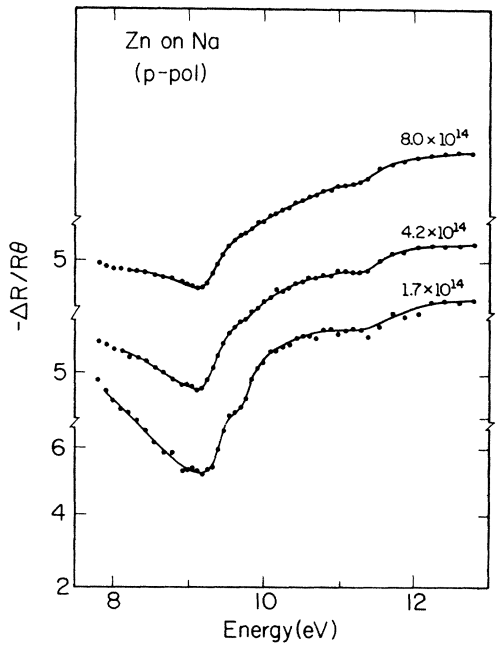

FIG. 4. Fractional reflectivity change, normalized as in Fig. 1, caused by impurities adsorbed on Na at various coverages.

with coverage and are an order of magnitude larger than random offsets which occasionally occur, so their origin in adsorbate processes is unambiguously identified. Similar effects, both in the existence of a continuum and the occurrence of interferences, have previously been identified in the same energy range, for halogen ions dispersed in alkali-metal host lattices. The Zn $4s^2 \rightarrow 4s4p$ excitation also produces a resonance in the Drude-like continuum, near $\hbar\omega = 2.5$ eV.

Both the normalized continuum and the normalized resonance are larger for Zn adsorbed on Li than on Mg, and they increase further for substrates formed from the heavier alkali metals. Figure 3 gives spectra for low coverages of Zn on Li. Whereas for Zn on Mg the dip has a coverage-independent minimum of $\Delta R/R\Theta \sim 1$, it is noticeable that for Zn on Li the dip minimum occurs at larger signal strengths despite the growth of the Fano-resonance amplitude. Thus the continuum increases somewhat faster than the resonance as the coverage is reduced. This quantitative distinction aside, the spectra of Zn on Li remains quite similar to those of Zn on Mg both in their general forms and in their coverage dependences. Figure 4 shows similar results for Zn on thin Na films, for which the magnitude of the continuum appears still larger. The coverage dependence and general structure of the Fano process is, however, clearly maintained.

Results for Zn adsorbed on K, Rb, and Cs are presented in Figs. 5, 6, and 7. Still stronger continuum absorption is apparent, particularly for K and Rb. Also, there is a striking modification of the behavior at higher energy, $\hbar\omega > 11$ eV, where the absorption now *de*creases with energy, rather than increasing as for Mg, Li, and Na substrates. The result is that the resonance takes on an appearance more like a peak near 11 eV than a dip near 9 eV. Figure 8 shows spectra for Zn on Cs taken with a LiF filter to demonstrate that the offset and resonance behavior are correctly determined, and are not artifacts of imperfect monochromatization. Further striking features are visible in the spectra of Zn on Cs at and above 11.8 eV

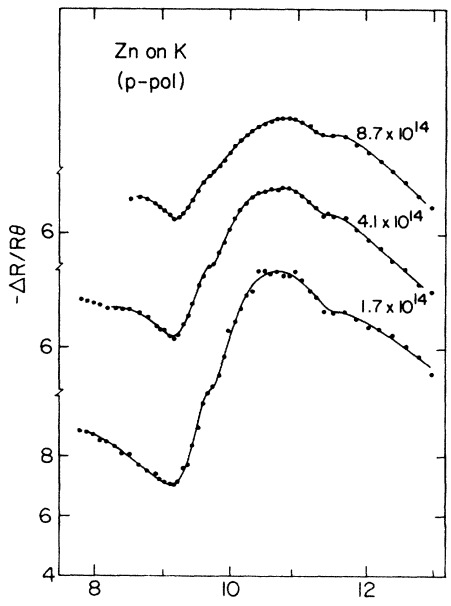

FIG. 5. Fractional reflectivity change, normalized as in Fig. 1, caused by impurities adsorbed on K at various coverages.

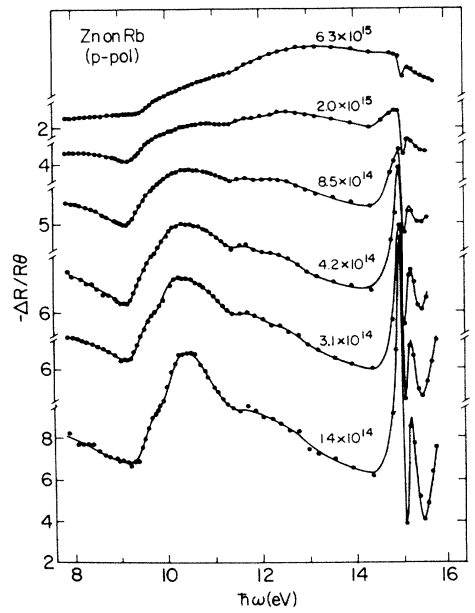

FIG. 6. Fractional reflectivity change, normalized as in Fig. 1, caused by impurities adsorbed on Rb at various coverages. The prominent features near 15 eV arise from the $N_{2,3}$ excitation of surface Rb atoms perturbed by the Zn impurities.

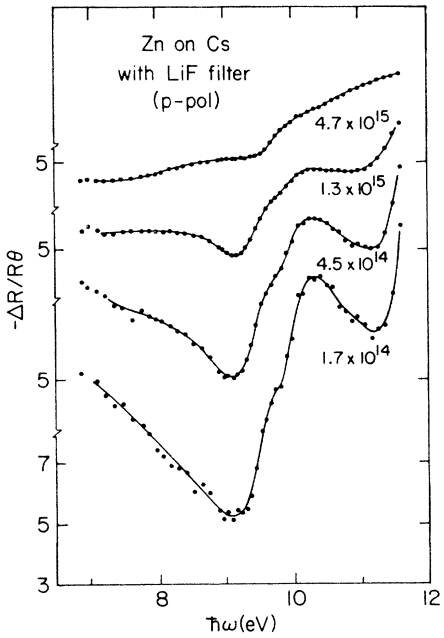

FIG. 8. Spectra of Zn on Cs, as in Fig. 7, taken with a LiF filter in the optical path to verify that second-order light plays no part in determining the observed spectra.

and on Rb at and above 15 eV. These arise from the $N_{2,3}$ excitations of surface Rb atoms and the $O_{2,3}$ excitations of surface Cs atoms.[23] They are nonetheless Zn-specific features, induced in the differential spectra by the Zn adsorbates. Apparently the Zn surface species perturb the outer core excitations of the Rb and Cs substrate atoms to which the Zn adhere. Quite similar effects have been observed with rare-gas atoms[24] and halogens atoms[25] adsorbed on alkali-metal surfaces.

The final data to be reported here involve dilute Zn-Na and Zn-Rb alloys. These are difficult experiments and the results are not fully satisfactory in the energy span covered. Figure 9 shows the available spectra. For both the Na and Rb solvents the resonance dip is followed by a

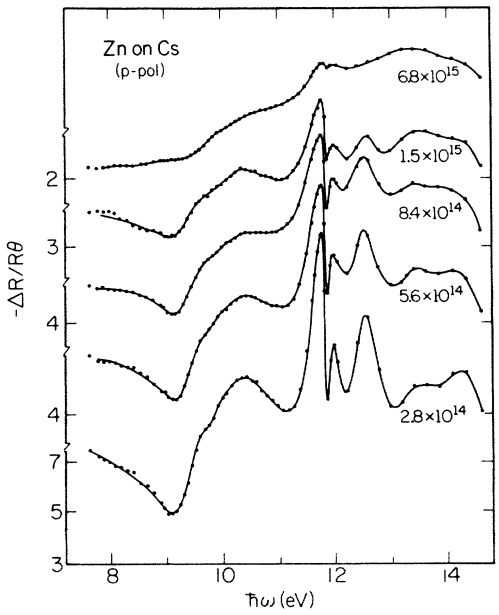

FIG. 7. Fractional reflectivity change, normalized as in Fig. 1, caused by impurities adsorbed on Cs at various coverages. The prominent feature near 12 eV arises from the $O_{2,3}$ excitation of surface Cs atoms perturbed by the Zn impurities.

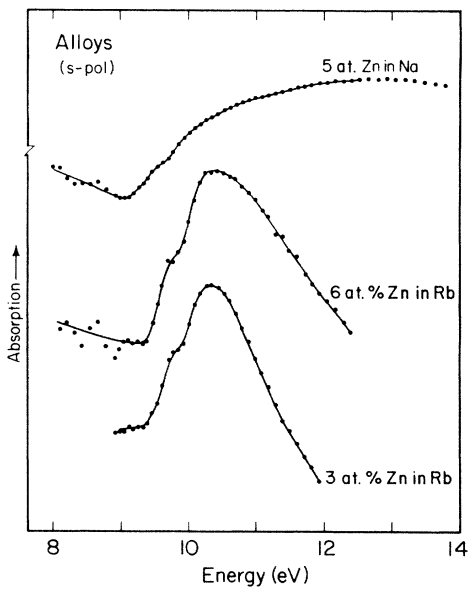

FIG. 9. Spectra of Zn alloyed into thin Na and Rb films at the concentrations indicated.

spin-orbit shoulder, just as in the adsorbate spectra. It is a striking fact, also, that the absorption above 11 eV increases with photon energy for the Na-based alloy, whereas for the Rb-based alloys the absorption decreases sharply with increasing energy. Thus the main qualitative features of the Zn spectra are closely parallel for the adsorbate and alloy systems.

IV. DISCUSSION

The purpose of this section is to discuss the experimental results presented above and to interpret them as far as seems possible at the present time. There are two main areas for consideration. In Sec. IV A, which follows immediately, the observed spectra are analyzed in a semiquantitative way to obtain experimental information about the processes involved in the $3d$-excitation region. Of particular interest, of course, are the continuum and local excitations, and the interferences the two exhibit. Similar phenomena have been observed by transmission[11] and ellipsometric methods,[12] and excellent "bulk absorption" spectra have been taken by reflectance methods from 3- to 5-monolayer films in this energy range,[21] so there is no reason to suppose that these observations are artifacts of the experimental method. Therefore, these phenomena must find their explanations in terms of the electronic structure of the metal-adsorbate or metal-impurity complex. Section IV B therefore considers the electronic structure of Zn atoms coupled to alkali-metal hosts. The discussion goes some way toward an identification of the continuum and local excitation processes, and provides a basic understanding of the interference characteristics deduced in Sec. IV A. Section IV C is a brief summary of the main results.

A. Analysis of spectra

Three aspects of the adsorbate spectra require careful attention. These are (i) the absorption continua and (ii) the interference processes, both observed in the limit of dilute coverage, and (iii) the way these characteristics change as the coverage is increases. A fourth area of interest is the relationship between the Zn spectra of the dilute alloys and the spectra of the analogous adsorbate systems. These are discussed consecutively in the present section.

Figure 10 provides a comprehensive view of alkali-metal-induced effects in Zn adsorbate spectra. There, the absorption spectra observed for the lowest Zn coverage on each alkali-metal substrate are compared on common scales of energy and amplitude. Note that the normalized spectra apparently remain coverage dependent (Figs. 3–9) even at the lowest doping levels reached in this work, so caution is needed in the interpretation. The results nevertheless reveal significant systematic trends.

It is convenient to consider the interference process first. An effort to fit the data with Fano profiles yield reasonable results, as shown in Fig. 11. The general features are illustrated there by reference to the examples of Zn on Na and Zn on Rb. In Fig. 11 the dotted line is a spin-orbit decomposition of the experimental curve, made assuming simple superposition. The tendency to oscillate

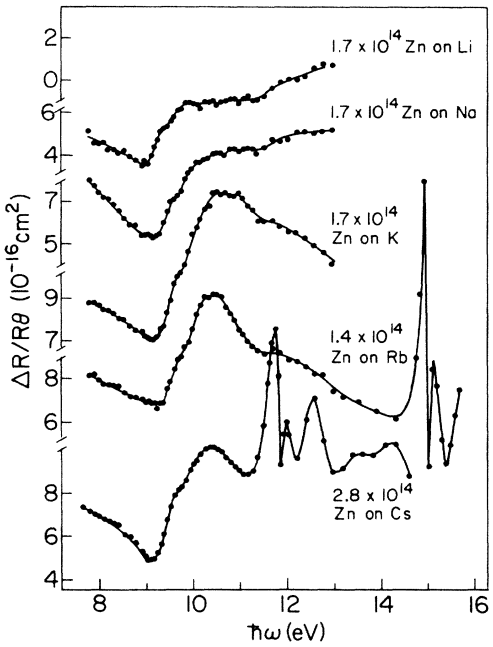

FIG. 10. Fractional reflectivity changes, normalized as in Fig. 1, caused by Zn adsorbed at dilution on Li, Na, K, Rb, and Cs. The normalized spectra apparently remained coverage dependent at the lowest coverages studied.

in the high-energy wing is probably an artifact of this procedure, but does not cause a major problem in the subsequent analysis. Dashed lines in Fig. 11 are fits of the Fano-Beutler profile

$$S(\hbar\omega)=A(q+\zeta)^2/(1+\zeta^2)\ .$$

Here, the photon energy $\hbar\omega$ is scaled and rezeroed to

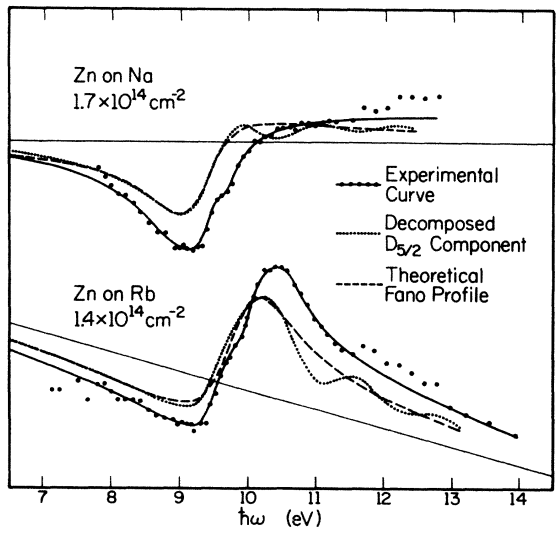

FIG. 11. Fits of Fano-Beutler profiles (solid lines) to the central parts of the $3d$ resonances of Zn adsorbed on Na and Rb. Parameters for the fit are given in Table I. Note that a sloping background is required for Rb.

TABLE I. Parameters for fits of Fano-Beutler profiles to Zn resonances in Fig. 3. Note that the decay width Γ varies by only $\sim 20\%$.

Zn	q	Γ (eV)	A (10^{-15} cm^2)	E_0 (eV)	$\langle l \rangle / \langle c \rangle$	Spin orbit (eV)	Ratio
Na	0.50	0.47	1.08	9.3	0.61	0.60	3:2
Rb	1.53	0.50	0.57	9.7	1.92	0.55	3:2
Na	0.60	0.60	1.25	9.3	0.82	0.60	3:2
Rb	1.70	0.55	0.95	9.75	2.23	0.50	3:2

$$\zeta = (\hbar\omega - E_0)/\Gamma \ ,$$

in which

$$\Gamma = \pi V^2$$

is the inverse lifetime of the excited configuration against decay into the continuum. The parameter q measures the optical matrix element $\langle l \rangle$ to the local state relative to that, $\langle c \rangle$, to the continuum:

$$q = |\langle l \rangle|^2 / \pi V^2 |\langle c \rangle|^2 \ .$$

In these expressions, V is the Coulomb matrix element for the decay and E_0 determines the energy shift caused by the interaction.

In order to obtain a reasonable fit for Zn on Rb it is necessary to employ a sloping background, as shown in Fig. 11. An adequate fit through the resonance region for Zn on Na can be made without a background bias, as shown in Fig. 11, but the fit deteriorates outside the central 4-eV range. The parameters q, Γ, A, and E_0 required by the data are collected in Table I, together with similar results for dilute alloys of Zn in Na and Zn in Rb (see below). All the fits employ reasonable spin-orbit splittings near 0.5 eV and an "ideal" ratio 3:2 between the $D_{5/2}$ and $D_{3/2}$ hole spectral amplitudes.[26] It is not possible by any combination of parameters to reproduce the sharpness of the inflection observed experimentally just below 10 eV. In the atom the $D_{5/2}$ and $D_{3/2}$ ($J=1$) channels interfere not only with the continua but with each other also, to produce a complex spectrum with an extremely sharp central dip.[2] The sharp inflection near 10 eV may signal a similar interference between the channels for the two core holes. This would not be simulated by the simple superposition employed in the construction of Fig. 11.

To begin an interpretation of the continuum we have been guided by the Fano fits as an indication of the background trends. Figure 12 sketches the general size and wavelength dependence of the continua so deduced for the light (L) alkali metals Na and Li, and for the remaining heavy (H) alkali-metal substrates. These have been drawn for the dilute limit, taking approximate account of the observed coverage dependences. The inferred spectra remain speculative in part because the data are limited in energy range and coverage. It nevertheless seems clear that the heavy alkali metals possess stronger continua which fall off rapidly above 9 eV, while the weaker continua for Li and Na extend out beyond 12 eV.

With respect to this general size of the resonance one may now note that it undergoes stronger fractional changes with coverage than the impurity-induced continuum, and in the same sense. Thus in passing from high to low coverage on any substrate (Figs. 3—8) the normalized continuum and the normalized resonance both increase, but the latter proportionally much more than the former. This is the case also in the comparison among substrates in Fig. 10 where, for K, the resonance and the continuum are largest, and, for the Li substrate, they are the smallest. These two amplitudes are thus interrelated in a way which transcends details of the environment which produces the continuum and resonance processes.

By far the most striking feature of the relationship between the continuum and the resonance, however, is their relative size. It is easy to see that the oscillator strength for the local state is less than the integrated strength of the impurity-induced continuum by more than an order of magnitude. Note that since these are differential measurements, the continuum referred to here is just the *change* induced by the impurities. Evidently this change is of very substantial size, being at least an order of magnitude greater in total oscillator strength than the sharp component of the fully allowed transition from the $3d$ full shell to the empty $4p$ shell. In all, the relationship of the Zn $3d$ resonance to its continuum is rather similar to the analogous behavior of halogen impurities in bulk alkali metals, as investigated by Avci and Flynn,[10] which display phenomena of the same type in transmission.

Remarkably similar features are evident in the few available spectra for Zn impurities in bulk alkali metals.

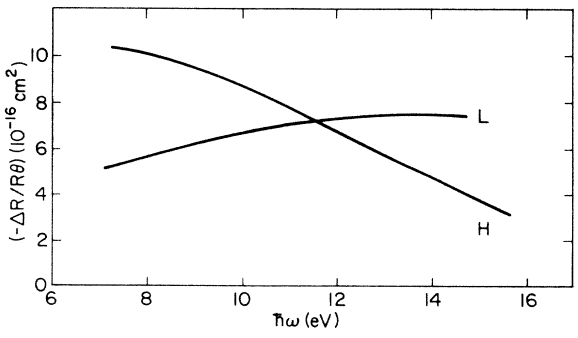

FIG. 12. Sketch indicating approximate Zn-induced continua for light- (L) and heavy- (H) alkali-metal host lattices.

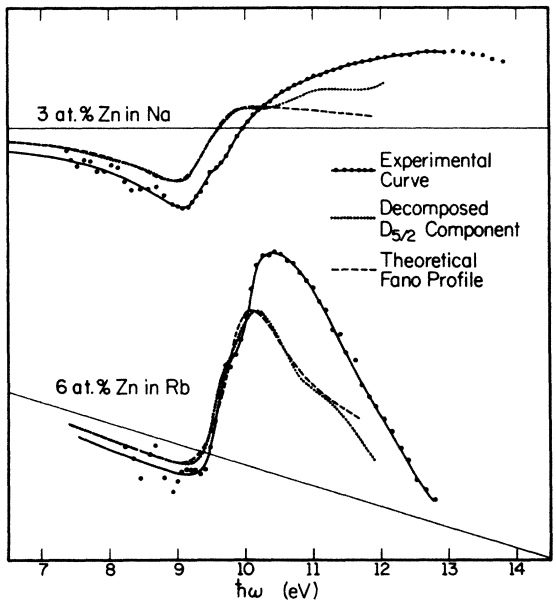

FIG. 13. Fits of Fano-Beutler profiles (solid lines) to the central parts of the $3d$ resonances of Zn dissolved in Na and Rb. Parameters for the fits are given in Table I. Note that a sloping background is required for Rb.

Figure 13 shows Fano-Beutler profiles fitted to observed spectra for Zn dissolved in Na and in Rb. The fits are not very satisfactory. However, the Rb substrate once more requires a strongly sloping background whereas Na does not. Furthermore, the resonance for the Na alloy has a much weaker shoulder at high energy than that for the Rb alloy, just as in the adsorbate cases. In these alloy spectra, also, it is not possible to fit the sharp inflection just below 10 eV by a simple superposition of assumed $D_{5/2}$ and $D_{3/2}$ channels. The final fitting parameters are given in Table I for both the alloy and adsorbate systems. These are interesting enough to warrant further detailed comment.

The results collected in Table I show that, within the assumption of 3:2 spin-orbit ratio, the spectra are best fitted by values of the spin-orbit splitting and linewidth, Γ, which are almost the same for alloys and adsorbate systems and for both the Na and Rb host lattices. The linewidth, for example, varies only from 0.47 to 0.60 eV, with values for the adsorbates perhaps 10—20% less on average than those for the alloys. The splittings all fall in the range 0.55 ± 0.05 eV, for which differences may not be significant. It therefore seems possible to deduce from the results that neither the spin-orbit splitting, nor the decay rate of the Zn $3d^9 4s^2 4p$ excitation into the surrounding continuum, is strongly affected by the details of the environment. The latter conclusion might appear surprising until it is recognized that the analogous autoionizing resonance of the free Zn atom has a lifetime broadening of ~ 0.2 eV. In this light, the apparent change of Γ from the alloy to the adsorbate is about one-third of the change from the alloy to the free atom, which appears reasonable. The main apparent fact is that the decay rate is affected only to a modest degree by the wave-function distortions caused by the environment of the excited Zn core.

Three effects contribute to the markedly different spectra of Zn on the heavy alkali metals K, Rb, and Cs from those for the light alkali metals Li and Na. Of these the first arises from the continuum which, for heavy alkali metals, falls off strongly above about 9 eV, as documented above. The two factors pertaining to the resonance itself are its center E_0 and the shape parameter q, which are seen in Table I to exhibit a specific dependence on the host metal. Thus the values of q are 0.50 and 0.60 for Zn adsorbed on Na and dissolved in Na, whereas the values for the Rb host metal are 1.53 and 1.70, respectively. The striking shape changes between Na and Rb evidently arise from the change by about a factor of 3 which takes place in q. The corresponding line centers for impurities and adsorbates are 9.3 and 9.3 eV for Na and 9.75 and 9.7 eV for Rb, which exhibit the same correlations as those for q.

The final topic for discussion is the absolute magnitude of the observed resonance and of the continuum with which it interferes. In the atom, the $4s\rightarrow$continuum excitations begin near 9.4 eV (Ref. 1) and the $D_{5/2}$ and $D_{3/2}$ hole excitations interfere with this continuum and with each near 11.4 eV.[2,3] The continuum itself is relatively weak near threshold. As a consequence, the resonance contains the largest proportion of the observable $3d$ oscillator strength.

Figures 3—10 show that the situation is markedly different in the alloys. The resonance appears as a substantial feature on the impurity-induced continuum, but nevertheless contains more than an order of magnitude less oscillator strength. One may inquire whether or not the resonance is reduced from that of the atom or whether, alternatively, the continuum is enhanced. As a practical matter we find that oscillator strengths for adsorbates reproduce very systematically with increasing coverage on a given substrate. From one substrate to a second having a different chemical character, however, the present methods indicate oscillator strengths which can differ by a factor ~ 2 from the mean. This variability discourages quantitative assessments of oscillator strength until a better theoretical understanding is available.

Given the uncertainties it is still possible to compare the order of magnitude of one signal with another. In examining earlier results published elsewhere we find that rare-gas (Ref. 24) and Cs (Ref. 21) adsorbates exhibit closely comparable integrated p^6 oscillator strengths, which both agree from one substrate to the next only to about a factor 2 from the mean. When compared to this mean strength of the p^6 core excitations on the same substrates, the d^{10} excitations of Zn appear relatively weak. We find the Zn resonance oscillator strength over the 3-eV interval of greatest response to be $\frac{1}{2}$ to 1 order of magnitude less than that of rare-gas or alkali-metal adsorbates, even for the most favorable case, namely Zn on K. We conclude that the resonance itself contains only a small fraction of the d^{10} oscillator strength. Instead, it is the continuum, an order of magnitude greater in integrated strength, which appears to contain transition moments appropriate to the full Zn $3d$ shell.

In summary of the above analysis we note that the Zn-induced continua for the light- and heavy-alkali-metal hosts differ. The former are weaker but extend up beyond 12 eV, whereas the stronger continua associated with heavy alkali metals fall off rapidly above 9 eV. The integrated continuum oscillatory strengths appear comparable in the two cases, and have the same order of magnitude as the expected strength of the full $3d$ shell. The resonances themselves interfere with the continuum but contain over an order of magnitude less oscillator strength. These general characteristics are similar to those reported earlier for halogens in alkali metals.[10] The Zn resonances differ between heavy- and light-alkali-metal hosts mainly through the parameter q, which measures the ratio of local to continuum optical matrix elements; this appears typically a factor of 3 larger for heavy alkali metals than for light alkali metals. There is a corresponding shift of the resonance center E_0. These factors are strikingly similar for alloys and adsorbate systems. Finally, the decay rate Γ from the local Zn excitation to the continuum changes only by a factor of ~ 2 from the resonance in the alloy to the excitation of the isolated atom, with an intermediate result for the Zn adsorbate resonance.

B. Electronic structure

Our purpose here is to discuss the electronic structure of Zn impurities coupled to alkali-metal hosts, with a view to explaining the experimental results described above. In particular, we wish to understand the position of the $d^{10} \rightarrow d^9 p$ resonance, its magnitude and shape, and the origins of the continuum with which it interferes.

For all the alloys and adsorbate systems studied, the Zn $3d^{10} \rightarrow 3d^9 4p$ resonance is significantly red-shifted from its observed position near 11.4 eV in the free atom. From photoemission investigations of Zn in Cu, a similar shift of the $d \rightarrow p$ process to 9.7 eV is observed.[16] This has been explained[27] in the following way. The Zn* $3d^9 4s^2 4p$ valence structure is almost identical with the Ga $3d^{10} 4s^2 4p$ ground state for most chemical purposes. Thus the excited state bonds in Cu like Ga, while the ground state, of course, binds like Zn. The expected energy difference in this "$Z+1$" model[28] is about 1.5 eV for the excitation energy in Cu. This simple model thus provides a very satisfactory explanation of the observed 1.7-eV shift of the Zn $3d \rightarrow 4p$ excitation. Stokes-shift phenomena are expected to be small by comparison.[28] It cannot be doubted that the same factors cause a similar red shift of the Zn excitation when the atom is coupled to the surface or the bulk of alkali-metal host lattices. In fact, the resonances appear to center in the energy range 9.2–9.7 eV, with shifts typically near 2 eV from that of the free atom. We can interpret these shifts as arising mainly from the extra bonding of the excited configuration to the host metal, over that of the ground configuration.

Using known atomic properties it is also possible to piece together a useful picture of the one-electron orbitals of the ground and excited Zn configurations in the metal host lattice. The main point for the ground state is that the Zn $4s^2$ orbitals are bound several eV below the conduction-band bottoms. For this reason the atomic levels are then relatively little perturbed. In the excited $4s^2 4p$ state, the $4s^2$ orbitals must lie still a little lower, but the $4p$ level is close to the conduction band. It mixes degenerately with conduction states in Na, Li, Mg, and Zn, but falls below the conduction bands of K, Rb, and Cs. Apparently this is the cause of the changes of the Zn Fano profile which distinguish the heavy-alkali-metal hosts so clearly from the light alkali metals. These phenomena are discussed more quantitatively in what follows.

Figure 14 places the Zn one-electron $4s$ levels with respect to the alkali-metal conduction bands on an absolute scale. Since the orbitals are deeply bound, the metal can only remain neutral if conduction electrons are repelled from each Zn center to leave the Zn cell largely unoccupied. The same structural features have also been recognized for the full p^6 outer levels of rare-gas impurities.[24] Accordingly, the Zn orbitals mainly experience a small potential change due to the dipole distribution of conduction electrons around the periphery of the Zn cell, and lie in the vacant cell at energies near their levels in the atom. We are concerned with degenerate mixing, for which the levels in question must be placed on the same absolute energy scale. In forming the metal, the alkali-metal band states start at the atomic levels and are lowered by the cohesive energy, while broadening, as the atoms are brought together to make the metal. These mean levels, and the free-electron bandwidths, are the basis by which the band states are introduced on the energy scale of Fig. 14. Similar arguments have been employed previously to discuss alkali-metal, rare-gas, halogen, and other impurities in alkali-metal host lattices and on their surfaces.[10,18,21,24,29] The bonding shifts of the Zn levels are estimated approximately by sharing the cohesion among the Zn valence states.

Dashed lines in Fig. 14 indicate the approximate atomic $4p$ levels, when occupied by $3d \rightarrow 4p$ or $4s \rightarrow 4p$ transitions, as judged by the ionization energy of that excited state.[1] A point of central interest is that the $4p$ level ap-

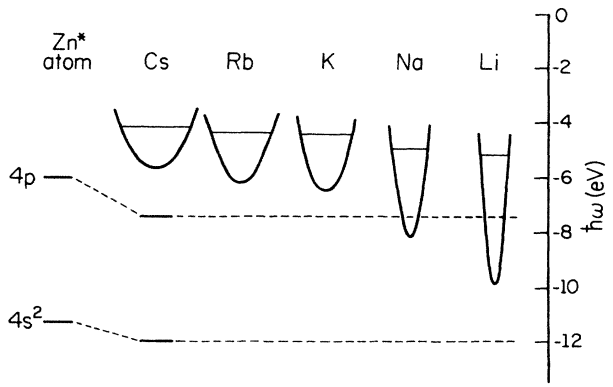

FIG. 14. Conduction bands of the alkali metals Cs, Rb, K, Na, and Li shown on the same energy scale as the occupied Zn $4s$ states (see text). The $4p$ levels, when occupied by $3d \rightarrow 4p$ or $4s \rightarrow 4p$ transitions, are indicated approximately by the dashed line. Note that degenerate mixing takes place between the $4p$ level and the Na and Li conduction-band states.

parently binds below the conduction-band bottom for Cs, Rb, and K metals, but is degenerate with band orbitals for Na and Li. The transition from bound to virtual levels with changing host metal coincides precisely with the change of the continuum and resonance behavior of the Zn $3d$ absorption, as documented above. A similar bound to virtual transition among alkali-metal hosts has been seen for alkali-metal impurities and adsorbates.[21,14]

Several excited configurations of the Zn impurity centers must be recognized in what follows. To shorten the discussion we again consider only a typical light host, characteristic of Li and Na, and a typical heavy host, characteristic of K, Rb, and Cs. For the latter case Fig. 15(a) shows an electron-hole pair excitation of the ground state, marked (e-h), the $3d^{10}4s^2 \rightarrow 3d^{10}4s4p$ excitation ($s \rightarrow p$), the $3d^{10}4s^2 \rightarrow 3d^9 4s^2 4p$ excitation ($d \rightarrow p$), and the $3d^{10}4s^2 \rightarrow 3d^9 4s^2 5p$ excitation ($d \rightarrow p'$). The symbol in the circle drawn in the conduction band specifies the local structure in the deformed electron liquid at the impurity center. V indicates that the impurity cell is vacant (bound states neutralize the impurity), etc. All these excited configurations can contain added electron-hole pairs. The diagram to the right of Fig. 15(a) indicates schematically the energies at which the electron-hole continua for these different local configurations begin. Figure 15(b) provides

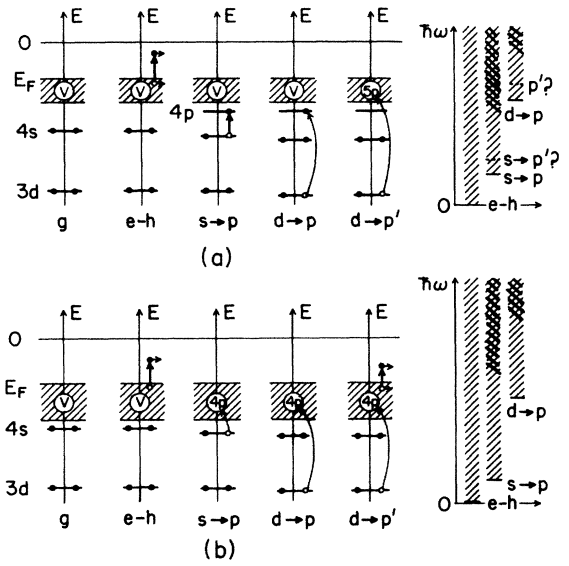

FIG. 15. Excited configurations of the impurity-metal complex for Zn interacting with (a) a heavy-alkali-metal host and (b) a light-alkali-metal host. Each figure sketches the ground state with an electron-hole pair excitation (e-h), the $4s \rightarrow 4p$ excitation ($s \rightarrow p$), the $3d \rightarrow 4p$ excitation ($d \rightarrow p$), and the $3d \rightarrow 5p$ excitation ($d \rightarrow p'$). The symbol in the circle indicates the local structure of the electron liquid in the self-consistent excited configuration. The $d \rightarrow p'$ excitation probably does not exist for light-alkali-metal hosts. In both (a) and (b) the drawing on the right indicates schematically the excitation continua derived from different locally excited configurations. Cross hatching indicates where the e-h continua may possibly be enhanced by the band p resonance.

similar information for the light-alkali-metal hosts. One principal difference is that the $4p$ level is a resonance in the conduction band for Li and Na.

The $4s^2 \rightarrow 4s4p$ excitation of Zn in Li has been reported elsewhere.[12] Like the $3d^{10}4s^2 \rightarrow 3d^9 4s^2 4p$ excitation, and for analogous reasons (see above), the $s \rightarrow p$ excitation is red-shifted by about 2 eV to $\hbar\omega \simeq 2.5$ eV. At this location the resonance sits on a strong continuum whose general characteristics are consistent with Drude processes for a reasonable order of magnitude of the impurity-induced conduction-electron scattering time.[12] For Zn impurities, however, the $4s^2 \rightarrow 4s4p$ resonance is very weak compared to the continuum. Moreover, the resonance decreases in amplitude and finally becomes submerged in the sloping Drude continuum as the Zn concentration is increased. These characteristics, determined by spectroscopic ellipsometry, appear to be closely analogous to the resonance-to-continuum ratio and concentration-dependent resonance strength reported in this work for the $3d^{10}4s^2 \rightarrow 3d^9 4s^2 4p$ excitation studied by differential reflectance. It is plausible to infer that these similarities must arise from the relationship of the $4p$ level to the conduction band, common to these two configurations, together with the general structure of the impurity, since the specific s and d core holes in the two configurations differ markedly in binding and in degeneracy. In the absence of conduction states, of course, all the resonances would be much sharper and the continuum would be greatly suppressed.

These experiments suggest two specific facts about local excitations coupled to a metallic host lattice. First, a large part of the oscillator strength may be taken from the local process and spread into a broad, diffuse continuum though the same energy range. Second, some part of the local excitation remains unaffected as a relatively sharp process related to the corresponding atomic event. It appears that the local portion may be reduced to 10% or less of the total strength, and that it is further suppressed when similar structures are located at neighboring sites. We know of no theory by which these characteristics may be modeled.[30]

If these inferences are correct, the (e-h) continua in Figs. 15(a) and 15(b) must be augmented by admixture of diffused portions of the main ($s \rightarrow p$) and ($d \rightarrow p$) excitations, to produce the observed impurity-induced continua (Fig. 12). The remaining portion of the local excitation evidently interferes with this continuum with the results visible in the optical data. Both the continua and the resonances change as the conduction band is modified through the series Cs to Li, and as the $4p$ level then merges into the conduction band. Thus the continuum spreads and the resonance weakens. In addition, the interference changes abruptly between K and Na as the p level enters the conduction band. Table I shows that no significant change takes place in the decay rate Γ from the local process to the continuum. However, the resonance center shifts in the direction of greater excited-state cohesion as the degenerate mixing occurs. Also, a change takes place in $q \sim \langle l \rangle / \langle c \rangle$, which decreases by a factor of 3. These same main features occur for the spectra of the alloy systems also.

Impurity-induced optical continua near $\hbar\omega = 10$ eV, of the type discussed above, have been observed only for Zn and halogen-ion impurities in alkali metals. Some explanation of this fact must be sought, but we can offer only qualitative indications of the possible causes. First, repulsive potentials produce a pattern of phase shifts η_l such that the local density of l wave states $N_l(E) = (2/\pi)(\partial\eta_l/dE)$ has a resonant peak at an energy given by a small multiple of E_F. This occurs for all repulsive scattering potentials at approximately the energy for which the band orbitals penetrate the repulsive barrier.[31] Zn is neutralized by bound $4s$ electrons and therefore repels band electrons from its cell. The $s \rightarrow p$ or $d \rightarrow p$ transitions to this band p resonance for Zn impurities (cross hatched in Fig. 15) may be the local electron-hole excitations which the core $d \rightarrow p$ resonance augments. Second, whereas the conduction-electron scattering time is $\sim 10^{-14}$ sec, the actual duration of conduction-electron impacts with the impurities may be $\sim 10^{-16}$ sec, which is the timescale relevant to the observed continua. Now as a conduction electron scatters abruptly from the repulsive impurity center, the strong interaction must have its counterpart in a distortion, or equivalently virtual excitations, of the impurity center. This is particularly so for highly polarizable centers like Zn and halogen ions. In this way, the collisions may possibly provide a mechanism by which the core excitations can become admixed with the conduction-band excitation processes to produce the type of oscillator-strength transfer reported in this research.

C. Summary

The work reported in this paper shows that a large proportion ($>90\%$) of the Zn $3d^{10}4s^2 \rightarrow 3d^9 4s^2 4p$ oscillator strength is diffused into an extended continuum when the Zn impurity interacts with alkali-metal host lattices. The continuum is weaker but more extensive for host metals like Li and Na, with E_F large, than for heavy alkali metals with E_F small. A sharp residue of the atomic process remains to interfere with the continuum at the location expected from "$Z+1$" arguments. Both the resonance and the continuum strength per impurity increase as the Zn concentration decreases. These phenomena resemble results reported earlier for halogen-ion and low-energy divalent atom excitations in alkali-metal hosts, except that the change in continuum strength with concentration is less noticeable in the earlier results.

At present there appear to be no theoretical models available by which these many-body processes can be described. At the time of this writing, a paper by Oliveria and Wilkins[32] has appeared which examines Fano processes in absorption for a resonant final state, although this is not precisely the process studied here. The basis of the work is a theory by Kotani and Toyozawa[33] which involves two excitation channels with differing screening distributions. It appears that any such theories need to be augmented by a more complete treatment of the continuum. Conduction-electron scattering from the impurities may possibly admix unbound components, or else the potential may induce a one-electron structure which contains local excitation resonances related to the observed optical continuum. Certainly, if the $4p$ orbital spreads appreciably in the metal, the oscillator strength of the local state is expected to decrease below that of the atom, so continuum portions must increase correspondingly. A substantial reduction of $q = \langle l \rangle / \langle c \rangle$ is observed to occur as the local state mixes with the continuum in passing from heavy- to light-alkali-metal hosts. None of these phenomena are understood quantitatively at present, however. There is a clear need for detailed theoretical investigations of these interesting many-body processes.

ACKNOWLEDGMENTS

We wish to thank J. E. Cunningham and D. L. Gibbs for their help with these experiments and for many stimulating discussions. This research was supported by the National Science Foundation (NSF) under Grant No. DMR-80-08139. Use of University of Illinois Materials Research Laboratory facilities supported by NSF Grant No. DMR-80-20250 is gratefully acknowledged. Thanks are due the staff of the University of Wisconsin—Madison Synchrotron Radiation Center at Stoughton, WI for their cooperation in the research.

---

*Present address: AT&T Bell Laboratories, Holmdel, NJ 07733.

[1]C. E. Moore, *Atomic Energy Levels,* U.S. National Bureau of Standards Circular (U.S. GPO, Washington, D.C., 1971).

[2]G. V. Marr and J. M. Austin, J. Phys. B **2**, 107 (1969).

[3]See, e.g., A. W. Fliflet and H. P. Kelly, Phys. Rev. A **10**, 508 (1974).

[4]U. Fano, Phys. Rev. **124**, 1866 (1961); U. Fano and J. W. Cooper, Rev. Mod. Phys. **40**, 441 (1968).

[5]For examples, see *X-Ray and Atomic Inner-Shell Physics—1982,* edited by B. Crasemann (AIP, New York, 1982).

[6]H. W. B. Skinner, Philos. Trans. R. Soc. London, Ser. A **239**, 95 (1940).

[7]T. Kobayashi and A. Morita, J. Phys. Soc. Jpn. **28**, 457 (1970).

[8]See, e.g., G. Wentin, Photoelectron Spectra **45**, 1 (1981), and references therein.

[9]G. P. Williams, G. J. Lapeyre, J. Anderson, R. E. Dietz, and Y. Yafet, J. Vac. Sci. Technol. **16**, 528 (1972).

[10]R. Avci and C. P. Flynn, Phys. Rev. Lett. **37**, 864 (1976); Phys. Rev. B **19**, 5981 (1979).

[11]L. I. Johansson, J. W. Allen, I. Lindau, M. H. Hecht, and S. M. B. Hagström, Phys. Rev. B **21**, 1408 (1980).

[12]G. A. Denton, M. Bakshi, and C. P. Flynn, Phys. Rev. B **26**, 3495 (1982); M. Bakshi, G. A. Denton, A. B. Kunz, and C. P. Flynn, J. Phys. F **12**, L235 (1982); M. Bakshi, G. A. Denton, C. P. Flynn, J. Boisvert, and A. B. Kunz, Phys. Rev. B **31**, 4972 (1985).

[13]See, for example, J. Ziman, *Principles of the Theory of Solids,* 2nd ed. (MIT Press, Cambridge, Mass., 1972).

[14]C. P. Flynn, Surf. Sci. **158**, 84 (1985).

[15]A. D. McLachlan, J. G. Jenkins, J. Liesegang, and R. C. G. Leckey, J. Electron Spectrosc. Relat. Phenom. **3**, 207 (1974).

[16]C. Norris and G. P. Williams, Phys. Status Solidi B **85**, 325 (1978).

[17]L. P. Mosteller, Jr. and F. Wooten, Phys. Rev. **171**, 743

(1968).

[18]T.-H. Chiu, J. E. Cunningham, Doon Gibbs, and C. P. Flynn, Phys. Rev. Lett. **52**, 388 (1984).

[19]J. E. Cunningham, D. K. Greenlaw, and C. P. Flynn, Phys. Rev. B **22**, 717 (1980).

[20]R. Avci and C. P. Flynn, Phys. Rev. B **19**, 5967 (1979).

[21]D. L. Gibbs, T.-H. Chiu, J. E. Cunningham, and C. P. Flynn, Phys. Rev. B **32**, 602 (1985).

[22]J. D. E. McIntyre and D. E. Aspnes, Surf. Sci. **24**, 417 (1971).

[23]See, for example, T. Ishii, Y. Sakisaka, T. Hanyu, H. Ishii, and S. Yamaguchi, J. Phys. Soc. Jpn. **42**, 876 (1977).

[24]D. L. Gibbs, J. E. Cunningham, and C. P. Flynn, Phys. Rev. B **29**, 5292 (1984); **29**, 5304 (1984).

[25]D. L. Gibbs, J. E. Cunningham, and C. P. Flynn (unpublished).

[26]Different ratios may occur in practice; see R. A. Pollack, S. Kawalczyk, L. Ley, and D. A. Shirley, Phys. Rev. Lett. **29**, 274 (1972).

[27]C. P. Flynn, J. Phys. F **10**, 315 (1980). Early use of this model was made by R. A. Tilton, D. J. Phelps, and C. P. Flynn [Phys. Rev. Lett. **32**, 1006 (1974)] for simple metals and B. Johannson [J. Phys. F **4**, 469 (1974)] for rare-earth metals.

[28]C. P. Flynn, Phys. Rev. Lett. **37**, 1445 (1976).

[29]T. H. Chiu, D. L. Gibbs, J. E. Cunningham, and C. P. Flynn, Phys. Rev. B **32**, 588 (1985).

[30]Note that the Anderson "orthogonality theorem" shows how determinantal configurations are diffused by one electron admixtures [P. W. Anderson, Phys. Rev. Lett. **18**, 1049 (1967)], while the "size consistency" problem occurs as many-body correlations reduce the amplitude of any determinantal configuration in the extended wave function of a solid [see E. R. Davidson and D. W. Silver, Chem. Phys. Lett. **52**, 403 (1977)].

[31]See, e.g., N. F. Mott and H. S. W. Massey, *The Theory of Atomic Collisions* (Pergamon, Oxford, 1965).

[32]L. N. Oliveira and J. W. Wilkins, Phys. Rev. **32**, 696 (1985).

[33]A. Kotani and Y. Toyozawa, Jpn. J. Phys. **37**, 912 (1974); **35**, 1073 (1973); **35**, 1082 (1973). See also K. Schönhammer and O. Gunnarson, Solid State Commun. **23**, 691 (1977); Phys. Rev. B **18**, 6606 (1978).